

Behavior of Railway Cars in Running (Report 2)

Seinosuke ARAI

Abstract

The stability of a railway car (vehicle) is discussed. The motion of a vehicle is analyzed as linear system at first, and then as non-linear system. Non-linear elements, such as friction, clearance, stopper, etc., influence the stability of railway vehicle in running. How to treat these non-linearities is explained.

Nomenclature

Notation	Unit	Definition
A	kgf·m/rad	real part of angular stiffness substituted for a describing function
A_0, A_1, \dots, A		coefficients of a characteristic equation
a	m	half length of wheel base
a_1	m	constant related to an amplitude of lateral vibratory displacement of a wheelset
a_2	m	constant related to an amplitude of lateral vibratory displacement of a wheelset
B	kgf·m/rad	imaginary part of angular stiffness substituted for a describing function
b	m	half distance between contact points of wheel treads and rails in the lateral direction
b_0	m	half spacing of bolster anchors in the lateral direction
b_1	m	half spacing of suspension mountings for a wheelset
b_2	m	half spacing of bolster springs in the lateral direction
c_{wx}	kgf·s/m	damping coefficient in the longitudinal direction (for an axle)
c_{wy}	kgf·s/m	damping coefficient in the lateral direction (for an axle)
c_z	kgf·s/m	damping coefficient in the vertical direction (conversion to bearing spring position, for an axle)
c_1	kgf·s/m	damping coefficient corresponding to k_1
c_2	kgf·s/m	damping coefficient corresponding to k_2
c_2'	kgf·s/m	damping coefficient corresponding to k_2'
F	kgf	tangential force; frictional force
F_{creep}	kgf	creep force
F_μ	kgf	frictional force
f	kgf	creep coefficient for a wheelset
G_B		vehicle body center of gravity
G_T		bogie frame center of gravity
G_W		wheelset center of gravity
g	m/s ²	acceleration of gravity
g_1	m	side clearance of an axle for an axle box

Received September 21, 1981

Notation	Unit	Definition
g_2	m	side clearance of an axle for an axle box
g_3	m	clearance between middle holder piece and lower holder piece of links
h_B	m	height of body center of gravity above axle center of wheelset
h_T	m	height of bogie frame center of gravity above axle center of wheelset
h_1	m	height of bolster spring center above bogie center of gravity
h_2	m	height of body center of gravity above the middle of bolster spring
I	kgf·m·s ²	moment of inertia of bogie in yaw
I_{Bx}	kgf·m·s ²	moment of inertia of half body in roll
I_{Bz}	kgf·m·s ²	moment of inertia of half body in yaw
I_{Tx}	kgf·m·s ²	moment of inertia of bogie frame in roll
I_{Tz}	kgf·m·s ²	moment of inertia of bogie frame in yaw
I_W	kgf·m·s ²	moment of inertia of wheelset in yaw
i_{Bx}	m	$=\sqrt{I_{Bx}/m_B}$; radius of gyration of half body in roll
i_{Bz}	m	$=\sqrt{I_{Bz}/m_B}$; radius of gyration of half body in yaw
i_{Tx}	m	$=\sqrt{I_{Tx}/m_T}$; radius of gyration of bogie frame in roll
i_{Tz}	m	$=\sqrt{I_{Tz}/m_T}$; radius of gyration of bogie frame in yaw
i_W	m	$=\sqrt{I_W/m_W}$; radius of gyration of wheelset in yaw
j		$=\sqrt{-1}$
k_t	kgf/m	gravitational stiffness for wheelset in the lateral direction due to difference between normal forces of wheels
k_i	kgf/m	equivalent value of k_t
k_{Wx}	kgf/m	longitudinal supporting stiffness of axle
k_{Wy}	kgf/m	lateral supporting stiffness of axle
k_z	kgf/m	vertical supporting stiffness of axle
k_0	kgf/m	bolster anchor stiffness
k_1	kgf/m	axle spring stiffness for half bogie
k_2	kgf/m	bolster spring stiffness for half bogie
k_2'	kgf/m	bolster spring lateral stiffness for half bogie
l	m	$=\sqrt{a^2+b^2}$; horizontal distance from bogie center to contact point between wheel and rail; half length of distance of bogie centers
M	kgf·m	moment
m	kgf·s ² /m	mass of bogie
m_B	kgf·s ² /m	half mass of vehicle body
m_T	kgf·s ² /m	mass of bogie frame
m_W	kgf·s ² /m	mass of wheelset
p	rad/s	$=\alpha+j\omega$; root of characteristic equation
r	m	radius of wheel tread circle
t	s	time
v	m/s	forward speed of vehicle
Y	m	amplitude in lateral
y	m	lateral axis
y_B	m	lateral displacement of vehicle body
y_T	m	lateral displacement of bogie frame (subscripts T1, T2 mean front bogie frame and rear one, respectively)
y_1	m	lateral displacement of front wheelset; lateral displacement of wheelset (mode 1)

Notation	Unit	Definition
y_2	m	lateral displacement of rear wheelset; lateral displacement of wheelset (mode 2)
α	rad/s	real part of characteristic number; damping factor; an exponent in calculation of tangential force
α_1	rad/s	real part of characteristic number
α_2	rad/s	real part of characteristic number
Γ_n		equivalent value of wheel tread inclination
γ		wheel tread inclination
λ	m	wave length of hunting
τ_{Wx}	s	$=c_{Wx}/k_{Wx}$; time constant of damping for k_{Wx}
τ_{Wy}	s	$=c_{Wy}/k_{Wy}$; time constant of damping for k_{Wy}
τ_z	s	$=c_2/k_2$; time constant of damping for k_z
Φ	rad	amplitude in roll
ϕ	rad	angular displacement
ϕ_B	rad	angular displacement of body in roll
ϕ_T	rad	angular displacement of bogie frame in roll (subscripts T1, T2 mean front bogie frame and rear one, respectively)
Ψ	rad	amplitude in yaw
ψ	rad	angular displacement
ψ_B	rad	angular displacement of body in yaw; turning angle of bogie at point B
ψ_E	rad	turning angle of bogie at point E
ψ_{max}	rad	maximum turning angle of bogie
ψ_T	rad	angular displacement of bogie frame in yaw (subscripts T1, T2 mean front bogie frame and rear one, respectively)
ω	rad/s	imaginary part of characteristic number; angular frequency
ω_1	rad/s	imaginary part of characteristic number; angular frequency
ω_2	rad/s	imaginary part of characteristic number; angular frequency

1. Introduction

The characteristic curves of lateral vibration for a 2-axle vehicle against advancing speed are shown as Fig. 1.1. It shows that when vehicle speed is given α_1 , ω_1 , α_2 and ω_2 are read from the figure. Then the formulas of the lateral vibration to the said speed is written as follows:

$$y_1 = a_1 e^{\alpha_1 t} \sin \omega_1 t \quad (1.1)$$

$$y_2 = a_2 e^{\alpha_2 t} \sin \omega_2 t \quad (1.2)$$

In each formula, if α is positive, the vibration is divergent or unstable, whereas if α is negative, it is convergent or stable. Though there are some modes of vibration other than these two, they are neglected because of their higher stabilities.

In Fig. 1.1, we see some of the curves of circular frequency (ω) do not change with vehicle speed, but some others change in proportion to vehicle speed. The former are the natural frequencies of the vehicle and the latter are the hunting frequencies of the wheelsets. The stability of vehicle motion changes from stable to unstable near the point of vehicle

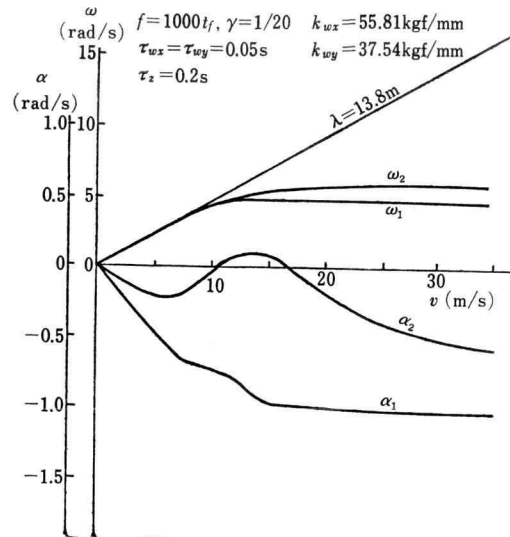


Fig. 1.1 Vibrational characteristics to the speed for a 2-axle railway vehicle

speed where the frequency of the hunting coincides with the natural frequency. The vehicle speed at which hunting appears for the first time, in changing the speed from low to high, is called the critical speed of hunting. The nature of the characteristics of vehicle with bogies is almost the same as a 2-axle vehicle. Thus the running stability is one of the important check points for railway vehicle to increase their operation speed.

On the subject of wheelset hunting, it has been studied for a long time since Klingel⁽¹⁾ discovered, in 1883, that the hunting was produced in kinematic way by the effect of conicity of wheel tread. He deduced also that the wave length of the hunting was inversely proportional to the square root of a gradient of the wheel tread. In 1937, Heumann⁽²⁾ deduced a calculation formula for a wave length of the hunting of wheelset whose wheel had a profile of circular arc instead of a straight gradient at the section. In 1953, Matsudaira⁽³⁾ solved the problem on the stability of railway vehicle as a self-excited motion by introducing the concept of creep between wheel tread and rail surface. Then he invented a double-link-suspension gear which makes the characteristics of vehicle superior in running stability. The conventional suspension gears of 2-axle freight vehicle were renewed, and their operation speeds were increased. This study on the stability of railway vehicle contributes to realize the high speed operation of the SHINKANSEN train.

The second chapter deals with an analysis of bogie vehicle (vehicle with bogies) through its equations of motion and one of the numerical solutions of the equation is explained. The progress of computer makes it possible to solve such a complex system of multi-degrees of freedom.

The third chapter deals one of the methods of stability analysis on bogie with non-linear elements. The non-linear elements influence the stability of railway vehicle in running. How to treat non-linearity is explained through an example.

2. Analysis of Lateral Motion of Railway Vehicles

One of the peculiarities of railway vehicles is to run on and along the settled rails. Wheels are guided by rails which have some irregularities in lateral and in vertical in the same way as a paved road has unevenness by which forced vibration of vehicle is produced. On the other hand, a wheelset (a pair of two wheels and an axle) itself has a character of producing self-excited vibration as mentioned on the Report 1. In this chapter the lateral motion of a vehicle with wheelsets is explained.

2.1 Stability of lateral motion of vehicle⁽⁴⁾

Standing tests for a whole vehicle and for a bogie with a dummy load corresponding to a half body of vehicle are schematically shown in Fig. 2.1. These tests are available as one of the effective means for experimental study on the hunting of vehicle. It is one of the most important problems on railway vehicles to prevent hunting motion. On this point of view, testing with this standing device before test running on service track is very effective with respect to safety, cost, labour and time.

It must be ideal to use a whole vehicle for the standing test. It would be, however, more economical if a single bogie could substitute for a whole vehicle. To this end, a comparison was made by numerical calculation both of a vehicle and of a bogie with a dummy load and a pivot around which the load can turn.

2.2 Equations of motion for a vehicle

By adding up the equations for front and for rear half of a vehicle⁽⁴⁾, we can get the equations for a whole vehicle as follows:

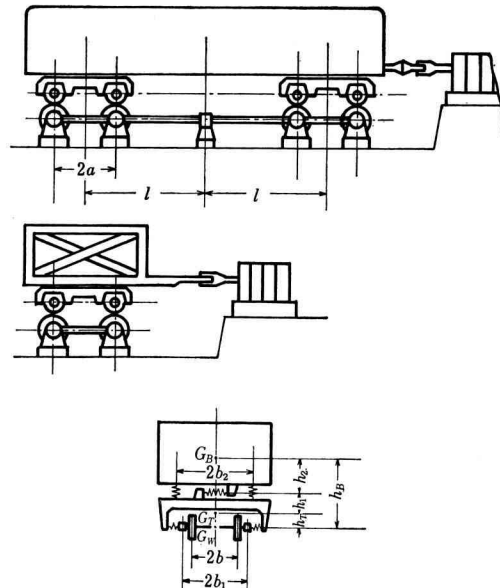


Fig. 2.1 Full scale test stand for a vehicle and for a bogie

$$\begin{aligned} \bar{m}_T \dot{y}_{T1} + 2f \left(\frac{\dot{y}_{T1}}{v} - \psi_{T1} \right) + 2k_t y_{T1} \\ + 2k_2' (y_{T1} - h_1 \phi_{T1} - y_B - l\psi_B - h_2 \phi_B) = 0 \end{aligned} \quad (2.1)$$

$$\begin{aligned} \bar{I}_{Tz} \ddot{\psi}_{T1} + 2f \left(\frac{a^2 + b^2}{v} \dot{\psi}_{T1} + \frac{b\gamma}{r} y_{T1} \right) \\ + 2a^2 k_t \psi_{T1} + 2b_0^2 k_0 (\psi_{T1} - \psi_B) = 0 \end{aligned} \quad (2.2)$$

$$\begin{aligned} I_{Tz} \ddot{\phi}_{T1} + 2b_2^2 k_2 (\phi_{T1} - \phi_B) + 2b_1^2 k_1 \phi_{T1} \\ - 2h_1 k_2' (y_{T1} - h_1 \phi_{T1} - y_B - l\psi_B - h_2 \phi_B) = 0 \end{aligned} \quad (2.3)$$

$$\begin{aligned} 2m_B \dot{y}_B - 2k_2' (y_{T1} - h_1 \phi_{T1} - y_B - l\psi_B - h_2 \phi_B) \\ - 2k_2' (y_{T2} - h_1 \phi_{T2} - y_B + l\psi_B - h_2 \phi_B) = 0 \end{aligned} \quad (2.4)$$

$$\begin{aligned} 2I_{Bz} \ddot{\psi}_B - 2b_0^2 k_0 (\psi_{T1} - \psi_B) - 2b_0^2 k_0 (\psi_{T2} - \psi_B) \\ - 2lk_2' (y_{T1} - h_1 \phi_{T1} - y_B - l\psi_B - h_2 \phi_B) \\ + 2lk_2' (y_{T2} - h_1 \phi_{T2} - y_B + l\psi_B - h_2 \phi_B) = 0 \end{aligned} \quad (2.5)$$

$$\begin{aligned} 2I_{Bz} \ddot{\phi}_B - 2b_2^2 k_2 (\phi_{T1} - \phi_B) - 2b_2^2 k_2 (\phi_{T2} - \phi_B) \\ - 2h_2 k_2' (y_{T1} - h_1 \phi_{T1} - y_B - l\psi_B - h_2 \phi_B) \\ - 2h_2 k_2' (y_{T2} - h_1 \phi_{T2} - y_B + l\psi_B - h_2 \phi_B) = 0 \end{aligned} \quad (2.6)$$

$$\begin{aligned} I_{Tz} \ddot{\phi}_{T2} + 2b_2^2 k_2 (\phi_{T2} - \phi_B) + 2b_1^2 k_1 \phi_{T2} \\ - 2h_1 k_2' (y_{T2} - h_1 \phi_{T2} - y_B + l\psi_B - h_2 \phi_B) = 0 \end{aligned} \quad (2.7)$$

$$\begin{aligned} \bar{I}_{Tz} \ddot{\psi}_{T2} + 2f \left(\frac{a^2 + b^2}{v} \dot{\psi}_{T2} + \frac{b\gamma}{r} y_{T2} \right) \\ + 2a^2 k_t \psi_{T2} + 2b_0^2 k_0 (\psi_{T2} - \psi_B) = 0 \end{aligned} \quad (2.8)$$

$$\begin{aligned} \bar{m}_T \dot{y}_{T2} + 2f \left(\frac{\dot{y}_{T2}}{v} - \psi_{T2} \right) + 2k_t y_{T2} \\ + 2k_2' (y_{T2} - h_1 \phi_{T2} - y_B + l\psi_B - h_2 \phi_B) = 0 \end{aligned} \quad (2.9)$$

where,

$$\bar{m}_T = m_T + 2m_W \quad (2.10)$$

$$\bar{I}_{Tz} = I_{Tz} + 2I_W + 2a^2 m_W \quad (2.11)$$

2.3 Numerical calculation and its results

Substituting $y = Y e^{pt}$, $\psi = \Psi e^{pt}$, $\phi = \Phi e^{pt}, \dots$, where $p = \alpha + j\omega$, $j = \sqrt{-1}$, into the equations of motion, and putting the determinant of a coefficient matrix of Y, Ψ, Φ, \dots , as zero we get a characteristic equation, and solving it by a computer, α and ω can be obtained for various speeds of vehicle.

The numerical data used for the calculation are as follows, and they are similar to those of the SHINKANSEN vehicle except k_0 .

$m_{Bg} = 19000$ (kgf),	$m_{Tg} = 6500$ (kgf),	$m_{Wg} = 1750$ (kgf)
$i_{Bz} = 7.24$ (m),	$i_{Tz} = 1.18$ (m),	$i_W = 0.73$ (m)
$i_{Bx} = 1.3$ (m),	$i_{Tx} = 1.00$ (m),	$f = 1315$ (tf)
$h_B = 1.295$ (m),	$h_2 = 0.915$ (m),	$h_1 = 0.18$ (m)
$l = 6.875$ (m),	$a = 1.25$ (m),	$b = 0.75$ (m)
$b_0 = 1.42$ (m),	$b_1 = 1.05$ (m),	$b_2 = 1.25$ (m)
$r = 0.455$ (m),	$\gamma = 1/40$,	$k_0 = 100000$ (kgf/m)
$k_1 = 259000$ (kgf/m),	$k_2 = 50000$ (kgf/m),	$k_2' = 36000$ (kgf/m)
$c_1 = 4000$ (kgf.s/m),	$c_2 = 2200$ (kgf.s/m),	$c_2' = 5000$ (kgf.s/m)

The results of the numerical calculation are shown in Fig. 2.2. The figure shows the characteristic curves of hunting, i.e., the variation of frequency and damping of lateral motion of a vehicle with speed. The upper group of curves gives the frequency ω and the lower one the damping factor α .

At the speeds of some 30 m/s and 50 m/s, the vibratory motion become less convergent, as seen in the figure. Beyond 90 m/s, α changes negative to positive which means the vibration diverges.

One way to find optimum combination of variable factors, is to assume the computing results as experimental data, and to apply them data processing. This way cannot be theoretically exact, but in a small range it will be practical as an engineering sense.

Thus the SHINKANSEN train has been running for over 15 years in stable and in safe.

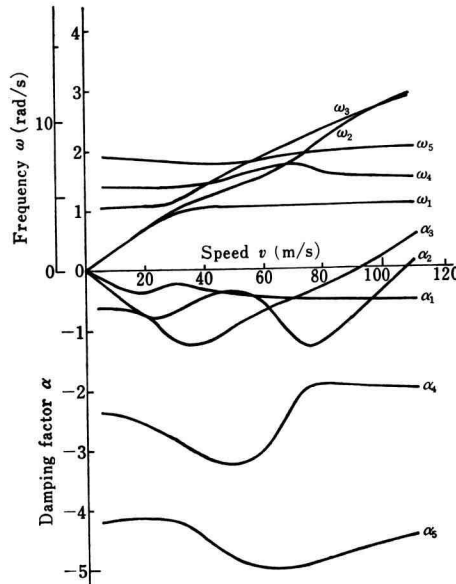


Fig. 2.2 Characteristic curves for a vehicle

3. Non-linear Elements of Railway Vehicles

As far as the last section, the analysis has been made by way of linear system, but there are many elements with non-linearity in regard to railway vehicles. This section states the non-linear elements of railway vehicles, and then shows the way to treat them using an example of non-linear stiffness of bogie turning, which affects the stability of hunting.

The non-linear elements, which affect the vibration of railway vehicles are mostly as the followings and their combinations.

- (1) clearance around bearing gears
- (2) friction, creep (small slippage between wheel and rail)
- (3) non-linear spring
- (4) non-linear damper

In the early stage of development of railway vehicle, clearance or friction might be given by chance, but nowadays they are used effectively by giving them suitable values which have been obtained by a long-time experience and by advanced analysis of vehicle motion.

Non-linearity of creep also influences in motion of vehicle. In case tangential force acts between running wheel and rail in the lateral direction, lateral creep is produced. The creep force, F_{creep} is expressed by

$$F_{creep} = -f \left(\frac{\dot{y}}{v} - \psi \right). \quad (3.1)$$

As the value of $\left| \frac{\dot{y}}{v} - \psi \right|$, which means the ratio of relative slippage between wheel and rail to running speed, increases, the tangential force F becomes smaller than creep force F_{creep} , and approaches to frictional force F_μ of slippage. Among these F , F_μ and F_{creep} , the following relation holds:

$$\frac{1}{F^\alpha} = \frac{1}{F_\mu^\alpha} + \frac{1}{|F_{creep}|^\alpha} \quad (3.2)$$

where α is a constant between 1 and 2. This formula is expressed by curve F in Fig. 3.1.

Double link mechanism of 2-axle car is an example of non-linear springs. Lateral stiffness of the mechanism is lowered by lengthening the equivalent length of links which connect vehicle body and bearing spring. A device of stopper between the upper and the lower link makes the lateral restoring force by double links larger as the amplitude of body relative to wheelset increases. When the amplitude become still larger, the motion of axle box is limited by a pair of axle box guarder or pedestal. As there is some clearance between journal of axle and plane bearing, when a wheelset moves laterally from neutral position, the clearance closes at first, a pair of double link moves, and then the lower link touches a stopper. As a result, the non-linear characteristics of force to lateral displacement of a wheelset is as shown in Fig. 3.2. This is an example that spring constant changes with the amplitude of spring deflection. In small amplitude of body lateral motion, stability of hunting is a factor to design spring constant and in large amplitude, limitation of body

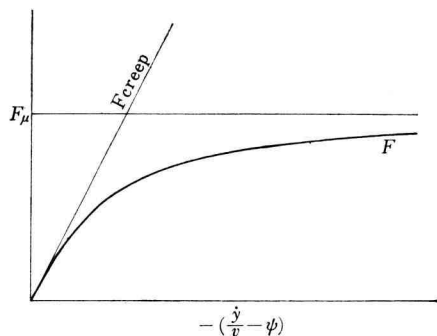


Fig. 3.1 Tangential force to creep force

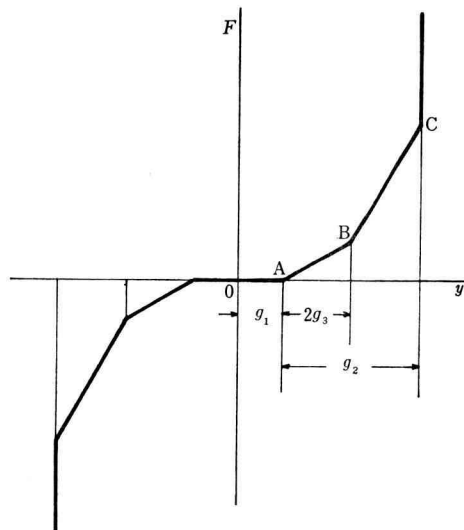


Fig. 3.2 Lateral force characteristics of double link suspension

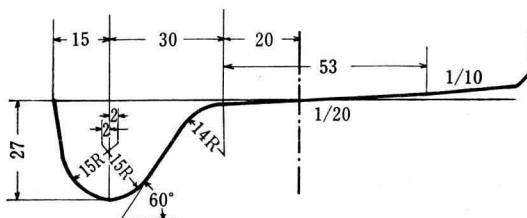


Fig. 3.3 Profile of conventional wheel tread

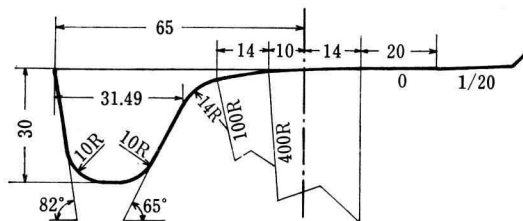


Fig. 3.4 Profile of N-tread

motion becomes an important factor.

A new non-linear profile of wheel tread⁽⁵⁾ has been developed for 2-axle cars with double link suspension to fulfill the conditions, that is, to increase safety against derailment, to improve hunting of body and to lessen wear of wheel tread. The tread is called N-type wheel tread, or N-tread. Figure 3.3 is the profile of conventional wheel tread, and Fig. 3.4 is that of N-tread, which is designed suitable for the 50N rail, Fig. 3.5. The improved points of N-tread for safety against derailment are the angle of wheel frame increased from 60 to 65 degrees, and the height of wheel frame increased from 27 mm to 30 mm, so that the height of the straight part of frame (point shifting to 15R at conventional tread, 10R at N-tread) increased from 19.5 mm to 25 mm.

Each gradient of tread of right and left wheel with N-tread is the same with the conventional wheelset at the neutral position, so the wheel load does not affect the lateral motion of wheelset. With the N-tread, on the other hand, difference arises between the gradients of right and left wheel treads as the wheelset moves in the lateral direction. The lateral restoring force produced by this difference makes the hunting of vehicle stable. Figure 3.6 shows the amplitude characteristics of the restoring stiffness \bar{k}_l and the equivalent

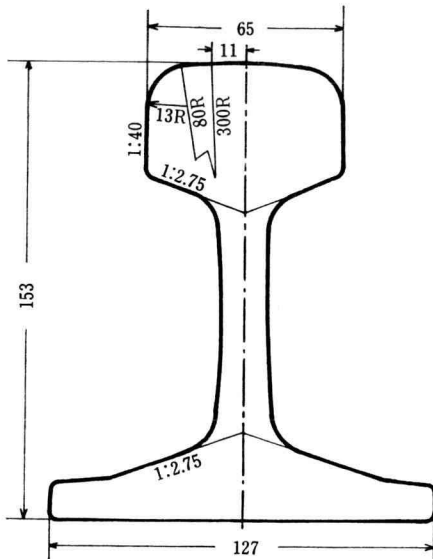


Fig. 3.5 Profile of 50N rail

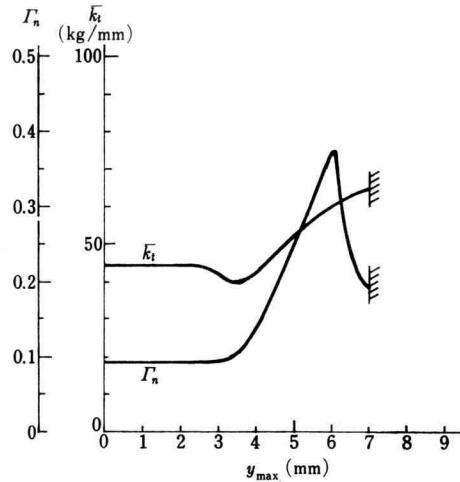


Fig. 3.6 Characteristics of N-tread to lateral amplitude

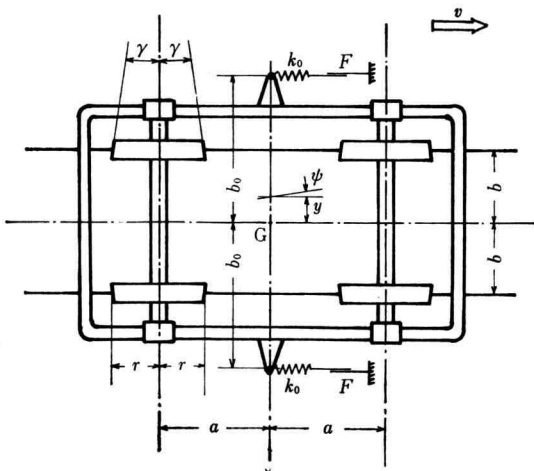


Fig. 3.7 Model of a bogie

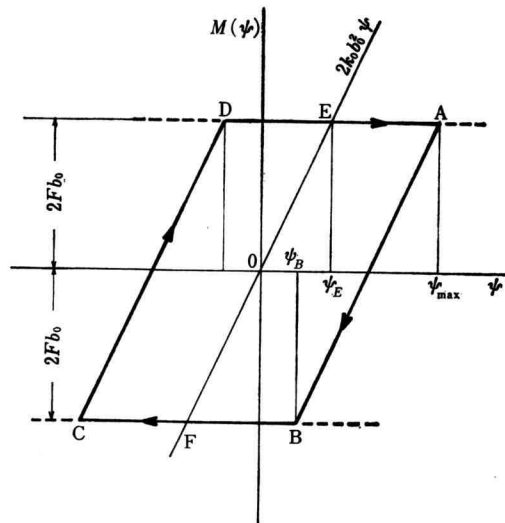


Fig. 3.8 Restoring moment to bogie turning angle

gradient of tread Γ_n , which is calculated by the wave length of kinematic hunting of the wheelset.

3.1 Stability of motion of bogie with non-linear element of turning^{(6),(7)}

To prevent the hunting of vehicle, it is a useful mean to provide frictional resistance against bogie turning with bogie side bearers. For an actual bogie, however, the

elastic deformation is inevitably found in the device for transmitting this frictional force from vehicle body to bogie. For instance, it is the deformation of rubber bushes put in at both ends of bolster anchor, or that of twist of bolster beam. Therefore, the frictional resistance against bogie turning will act as a combination with spring in series, which is schematized in Fig. 3.7. When bogie hunting is in a steady state, the relation between turning angle of bogie and moment will be expressed as Fig. 3.8. It is one of the most important problems of bogie design how to fix the amount of elasticity and frictional force.

The bogie model for the analysis is as Fig. 3.7. It is assumed that the vehicle body is standing still, all lateral forces acting between body and bogie are neglected, and only the moment of turning bogie around vertical axis is provided by the combination of spring and friction in series. Wheelsets are supposed to be fixed stiff to bogie frame in longitudinal and in lateral. The linear creep is applied to the slippage between wheel tread and rail, and neglecting the repulsion action of wheel flange against rail, the lateral motion of bogie can be expressed by the following equations:

$$\left. \begin{aligned} m\ddot{y} + 2\frac{f}{v}\dot{y} - 2f\psi &= 0 \\ I\ddot{\psi} + 2\frac{f}{v}l^2\dot{\psi} + 2f\frac{b\gamma}{r}y &= -M(\psi) \end{aligned} \right\} \quad (3.3)$$

where y for lateral displacement of bogie center, ψ for angular displacement of bogie in yaw, and $M(\psi)$ for restoring moment by friction and spring.

As it can be seen in Fig. 3.7, if the turning angle ψ is small, the restoring moment $M(\psi)$ is proportional to ψ , but if the ψ reaches a certain value there occurs slipping at side bearers and $M(\psi)$ holds the frictional moment. And when the bogie is in steady

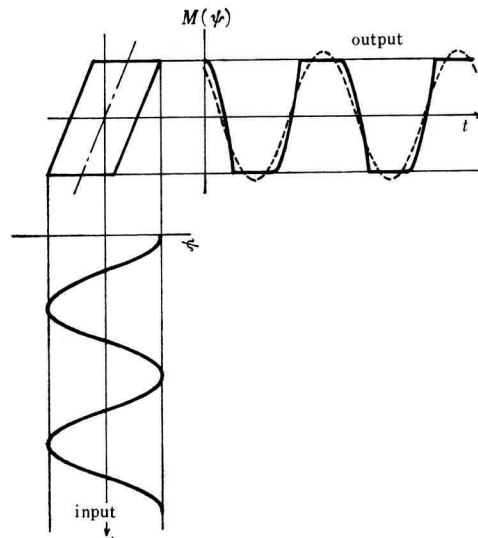


Fig. 3.9 Relation between input and output wave form for a system with hysteresis

vibration, the force at side bearer describes a hysteresis curve as shown in Fig. 3.8. This means that a sinusoidal input of ψ changes to a wave expressed by output of $M(\psi)$ as full line in Fig. 3.9.

The dotted line is a basic wave of Fourier expansion of $M(\psi)$, and this wave is somewhat advancing in phase compared with the wave ψ . So the moment can be expressed approximately by the real part of the following:

$$\bar{M}(\psi) = (A - jB) \psi \quad (3.4)$$

Putting, $\psi = \psi_{\max} e^{j\omega t}$

$$\begin{aligned} \bar{M}(\psi) &= (A - jB) \psi_{\max} e^{j\omega t} \\ &= [A\psi_{\max} \cos \omega t + B\psi_{\max} \sin \omega t] \\ &\quad + j[A\psi_{\max} \sin \omega t - B\psi_{\max} \cos \omega t] \end{aligned} \quad (3.5)$$

This shows that the real part of $\bar{M}(\psi)$ is a basic wave of Fourier expansion. Thus the non-linear equations (3.3) can be replaced by the linearized equations as follows:

$$\left. \begin{aligned} m\ddot{y} + 2\frac{f}{v}\dot{y} - 2f\psi &= 0 \\ I\ddot{\psi} + 2\frac{f}{v}l^2\dot{\psi} + 2f\frac{b\gamma}{r}y + (A - jB)\psi &= 0 \end{aligned} \right\} \quad (3.6)$$

The solution of equations (3.3) will be analogized by that of these linearized equations.

The following equation is obtained by eliminating ψ in equations (3.6).

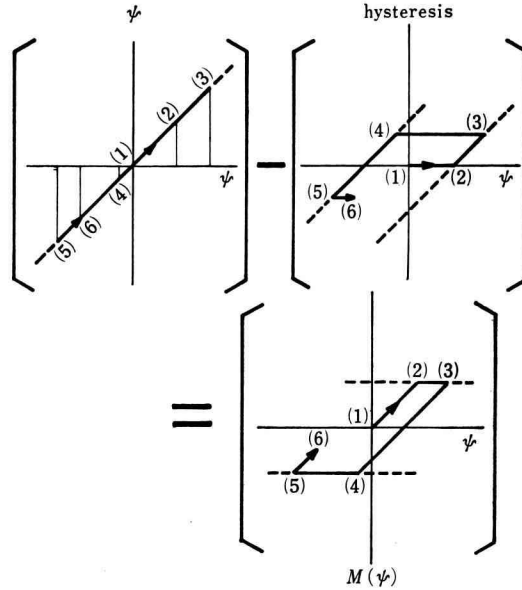
$$A_4 \ddot{\ddot{y}} + A_3 \ddot{\ddot{y}} + A_2 \ddot{\ddot{y}} + A_1 \dot{\ddot{y}} + A_0 y = 0 \quad (3.7)$$

where

$$\left. \begin{aligned} A_4 &= mI \\ A_3 &= 2\frac{f}{v}(I + ml^2) \\ A_2 &= 4\frac{f^2}{v^2}l^2 + m(A - jB) \\ A_1 &= 2\frac{f}{v}(A - jB) \\ A_0 &= 4f^2\frac{b\gamma}{r} \end{aligned} \right\} \quad (3.8)$$

It is rather difficult to solve analytically a non-linear differential equation as above-mentioned whereas an analogue computer is suitable and effective for that purpose.

$M(\psi)$ in the second equation of (3.3) is an expression of restoring moment against turning of bogie. $M(\psi)$ increases linearly with increasing of ψ , and after reaching the value of frictional moment, it keeps the constant value. Then, when ψ begins to decrease, $M(\psi)$ decreases. This characteristics is expressed as the downward figure in Fig. 3. 10, where

Fig. 3.10 Composition of $M(\psi)$

the abscissa is ψ and the ordinate is $M(\psi)$. For changing of ψ , from $0 \rightarrow \text{increase} \rightarrow \text{decrease} \rightarrow \text{increase}$, $M(\psi)$ goes along a pass (1) \rightarrow (2) \rightarrow (3) \rightarrow (4) \rightarrow (5) \rightarrow (6). The absolute values of $M(\psi)$ at (2) \rightarrow (3) and (4) \rightarrow (5) is equal to the moment by frictional force. In computer program, the characteristics of $M(\psi)$ can be obtained, as shown in Fig. 3.10, by subtracting hysteresis or backlash from input ψ .

Taking up a prototype bogie for the SHINKANSEN as an explanatory example, we use the following data:

$$\begin{array}{lll}
 m = 1107 \text{ (kgf.s}^2/\text{m)}, & I = 1869 \text{ (kgf.m.s)}, & a = 1.25 \text{ (m)} \\
 b = 0.75 \text{ (m)}, & b_0 = 1.415 \text{ (m)}, & l = \sqrt{a^2 + b^2} = 1.451 \text{ (m)} \\
 r = 0.455 \text{ (m)}, & \gamma = 1/40, & f = 1680 \times 10^3 \text{ (kgf)} \\
 k_0 = 100 \times 10^3 \text{ (kgf/m; variable)}, & & F = 500 \text{ (kgf; variable)}
 \end{array}$$

Denoting machine time by τ , real time by t , transformed displacement by Y and transformed angular displacement by Ψ , and making transformation of

$$\tau = 5t, \quad Y = 100y, \quad \Psi = 500\psi \quad (3.9)$$

we obtain the following equations by substituting (3.9) for (3.3):

$$\left. \begin{aligned}
 Y'' &= -607.0 \left(\frac{1}{v} \right) Y' - 24.28 \Psi \\
 \Psi'' &= -757.0 \left(\frac{1}{v} \right) \Psi' - 14.82 Y - M(\Psi)
 \end{aligned} \right\} \quad (3.10)$$

where ' represent differentiation for τ ,

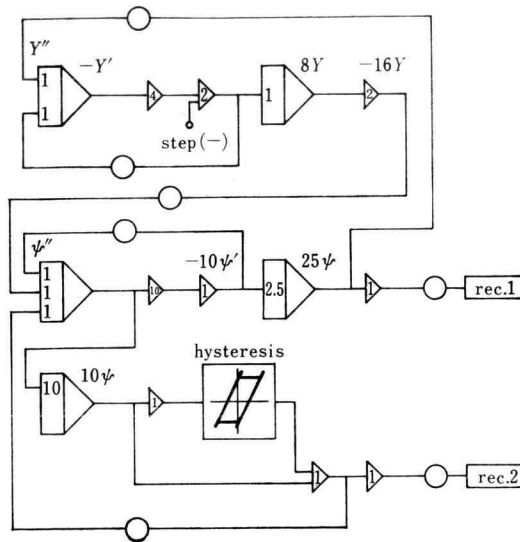


Fig. 3.11 Block diagram for bogie motion

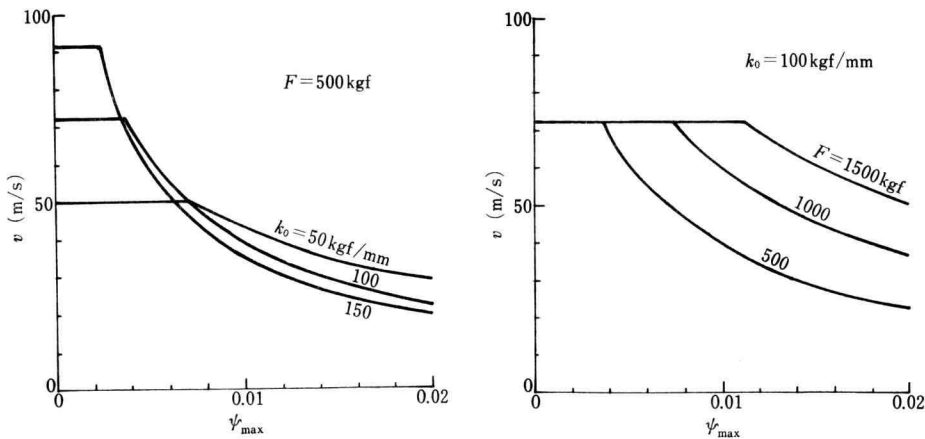


Fig. 3.12 Bogie hunting speed to bogie turning angle

$M(\Psi) = 8.570(\Psi - \Psi_0)$ and $|M(\Psi)| \leq 15.14$, Ψ_0 is constant when $|M(\Psi)| < 15.14$, but changes with Ψ to hold $|M(\Psi)| = 15.14$ if $|M(\Psi)|$ inclines to exceed the value.

The block diagram for analogue computation of (3.10) is shown in Fig. 3.11. Execution results are as Fig. 3.12, concerning maximum angular amplitude and critical speed of bogie hunting.

The results of analogue computation make clear that the frictional force by itself is not sufficient to restrain the bogie hunting, and that spring stiffness makes the critical speed of hunting high and the frictional force plays an important role to extend the range of spring effect in angular amplitude.

To obtain suitable values of the spring stiffness and the frictional force, it is necessary to give an additional consideration on the effect of suspension stiffness of wheel axle against bogie frame in the lateral or longitudinal direction, which is one of the main factors in bogie hunting.

4. Remarks

The author wishes to review on the behavior of railway vehicle in running, especially from the viewpoints of stability and safety on derailment. The materials for the review were chosen mainly from the reports which the author was related as a collaborator.

On this report, stability of railway vehicle as a linear system is explained which was effectively used for designing high speed vehicle. And one of the methods of handling non-linear system of railway vehicle bogie is also shown.

On the following report, computer simulation on railway vehicle derailment will be taken as well as an example of its application to derailment accident for making its causes clear.

References

- 1) Klingel: "Über den Lauf der Eisenbahnwagen", Organ Fortschr. Eisenb. -wes. **38** (1883)
- 2) Heumann: Organ Fortschr. Eisenbahn Wesen, **92** (1937), p 149
- 3) T. Matsudaira: "Nosing of 2-axle Railway Cars and its Prevention", First~Third Reports, Transactions of the Japan Society of Mechanical Engineers, 19-87 (1953), p 139~157 (in Japanese)
- 4) T. Matsudaira, N. Matsui, S. Arai, K. Yokose: "Problems on Hunting of Railway Vehicle on Test Stand", Transactions of the ASME Journal of Engineering for Industry, Aug. 1969, p 879 ~890
- 5) K. Yokose: "Wheel Tread Profile Suited for 2-axle Railway Vehicles", Lecture of Report, No. 232 Lecture Meeting, Kansai Branch, JSME, Jun. 8, 1974 (in Japanese)
- 6) T. Matsudaira, S. Arai, K. Yokose: "Combined Effects of Frictional and Elastic Moments Against Truck Turning upon Hunting of Truck", Railway Technical Research Report, No. 512, RTRI, JNR, Dec. 1965 (in Japanese)
- 7) K. Mano, S. Arai, K. Yokose: "Computer Solution for the Characteristics of the Nonlinear Hunting Vibration of Railway Vehicle Truck by Describing Method", Railway Technical Research Report, No. 602, RTRI, JNR, Jul. 1967 (in Japanese)